We are IntechOpen, the world's leading publisher of Open Access books Built by scientists, for scientists

4,800
Open access books available

122,000
International authors and editors

135M
Downloads

Our authors are among the

154
Countries delivered to

TOP 1%
most cited scientists

12.2%
Contributors from top 500 universities

CLARIVATE ANALYTICS BOOK CITATION INDEX INDEXED

WEB OF SCIENCE™

Selection of our books indexed in the Book Citation Index in Web of Science™ Core Collection (BKCI)

Interested in publishing with us?
Contact book.department@intechopen.com

Numbers displayed above are based on latest data collected.
For more information visit www.intechopen.com

Chapter 2

Thermal Inertia-Based Method for Estimating Soil Moisture

Dai Matsushima

Additional information is available at the end of the chapter

http://dx.doi.org/10.5772/intechopen.80252

Abstract

Thermal inertia is a parameter that characterizes a property of soil that is defined as the square root of the product of the volumetric heat capacity and thermal conductivity. Both properties increase as soil moisture increases. Therefore, soil moisture can be inversely determined using thermal inertia if a relationship between the parameters is obtained in advance. In this chapter, methods for estimating surface soil moisture using thermal inertia are comprehensively reviewed, with emphases on the followings: How thermal inertia is retrieved accurately from a surface heat balance model, and how it is accurately converted to surface soil moisture. In addition, the advantages and disadvantages of the thermal inertia methods are discussed and compared to microwave-based methods, such as spatial resolution and the sky conditions. Precise and accurate data from earth observing satellites are indispensable for estimating the spatial distribution of thermal inertia at a high resolution. On the other hand, data assimilation methods are rapidly developing, which may be competitive with thermal inertia methods. Finally, applications of thermal inertia methods are described and discussed for future explorations, such as dust emission in relation to soil moisture, and estimating regional water budgets by combining other satellite data.

Keywords: thermal inertia, soil moisture, thermal-infrared band, land surface temperature, earth observing satellite, surface heat balance, force-restore model, Fourier series expansion, microwave-based method

1. Introduction: thermal inertia of unsaturated soil

Thermal inertia P is one of the parameters used to characterize the thermal properties of soil and is defined as the square root of the product of the volumetric heat capacity C and thermal conductivity λ, which is given as

$$P = \sqrt{C\lambda}. \tag{1}$$

Thermal inertia appears in the formulation of the ground heat flux when it is formulated with a unique variable known as the land surface temperature (LST), and one does not have to consider the vertical profile of the soil temperature.

In terms of the relation between soil thermal properties and soil moisture, both the volumetric heat capacity C, which is the product of specific heat c and the bulk density ρ of the soil, and the thermal conductivity λ increase as the soil moisture increases. Accordingly, thermal inertia P also increases as soil moisture increases. Therefore, soil moisture can be estimated inversely if the thermal inertia value is known (**Figure 1**). The volumetric heat capacity is a moderate linear function of soil moisture [1]. By contrast, thermal conductivity has a strong nonlinearity with soil moisture, making it difficult to parameterize thermal conductivity and hence thermal inertia.

Thermal inertia is effective when the time series of the surface temperature is available, but the vertical profile of the soil temperature is not available. The differential equation for heat diffusion is given as

$$\frac{\partial T(z,t)}{\partial t} = \frac{\lambda}{C}\frac{\partial^2 T(z,t)}{\partial z^2}, \tag{2}$$

where $T(z,t)$ is the soil temperature at depth z and time t, which is the difference from a constant value at an infinite depth. This equation is solved to reproduce the daily and yearly

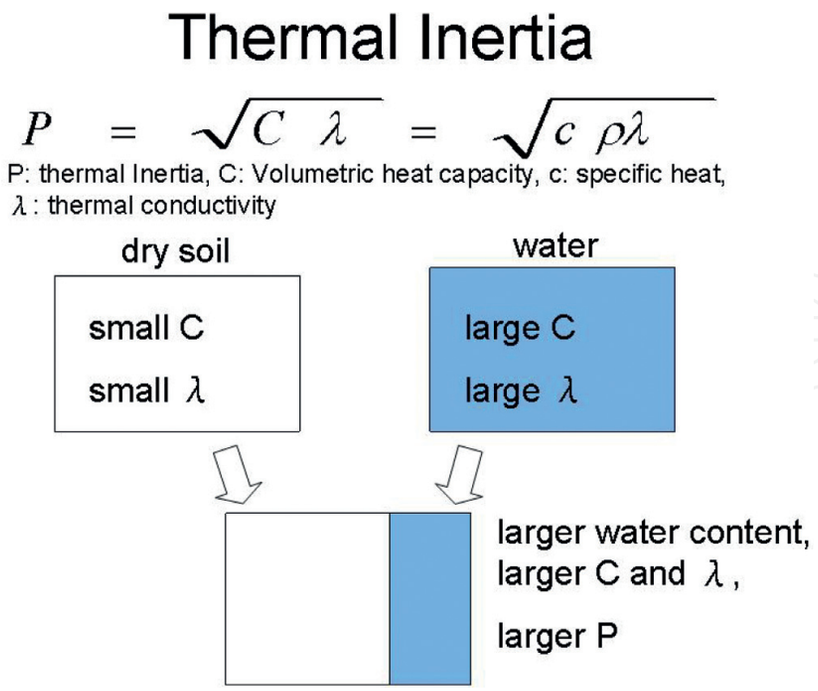

Figure 1. Schematic of the relationship between volumetric heat capacity, thermal conductivity, and thermal inertia in terms of soil moisture.

periodic cycles of soil temperature, under the boundary conditions that the temperature change is sinusoidal at the surface and constant at an infinite depth. The basic solution is as follows using the complex number expression:

$$T(z,t) = A\exp\left(-\frac{z}{d}\right)\cdot\exp\left[i\left(\omega t-\frac{z}{d}\right)\right], \tag{3}$$

if the surface boundary condition is $T(0,t) = A\cdot\exp[i\omega t]$. In Eq. (3), A is the amplitude of a periodic change with an angular velocity ω, d is the scale depth at which the amplitude is e^{-1} of the surface value, and i is the imaginary number $\sqrt{-1}$. The scale depth d is formulated as

$$d = \sqrt{\frac{2\lambda}{\omega C}}. \tag{4}$$

Eq. (3) is rewritten as follows using the real number expression:

$$T(z,t) = A\exp\left(-\frac{z}{d}\right)\cdot\cos\left[\omega t-\frac{z}{d}\right], \tag{5}$$

if the surface boundary condition is $T(0,t) = A\cdot\cos\omega t$.

The conductive heat flux in soil at depth z and time t, $G(z,t)$, is defined as

$$G(z,t) = -\lambda\frac{\partial T(z,t)}{\partial z}, \tag{6}$$

where the vertical profile of soil temperature is obviously required to calculate the soil heat flux. However, when the soil temperature solution (3) or (5) is applied to the soil heat flux Eq. (6) and then z is set to zero, it only uses the time series of surface temperature as follows:

$$G(0,t) = \sqrt{\frac{C\lambda}{2\omega}}\left[\frac{\partial T(0,t)}{\partial t}+\omega T(0,t)\right]. \tag{7}$$

In deriving Eq. (7), the following relation derived from Eq. (3),

$$\frac{\partial T(z,t)}{\partial t} = i\omega T(z,t), \tag{8}$$

is used. Eq. (7) is known as the force-restore method (FRM) for calculating the surface soil heat flux [2]. In Eq. (7), the numerator of the parameter is defined as thermal inertia P, which is given as

$$P = \sqrt{C\lambda} = \sqrt{c\rho\lambda}. \tag{9}$$

The above derivation describes thermal inertia being effective for quantifying soil thermal properties when only the LST is known, which leads to the analysis of the land surface processes using satellite LSTs. The above procedure leads to the studies proposed by Matsushima and co-researchers, which are described in Section 2.

Considerable effort has been made to estimate the thermal inertia of the Earth's surface mainly using LST data from satellites. Most of this effort has been concentrated on retrieving daily values of thermal inertia due to the availability of daily maximum and minimum LSTs observed from polar orbiting or geostationary satellites. Models using these types of satellite LSTs are based on the Earth's surface energy balance principle, which includes not only the radiation budget but also turbulent heat flux. A Fourier series expansion was introduced to solve Eq. (1) under the above Earth's surface boundary conditions using the solution of the real number expression, Eq. (5). Models have been improved from those using only the two daily extreme LSTs [3–8] to those using LSTs that are irrespective of time in a diurnal change [9, 10] and other significant studies that follow a series of important proposals by Xue and Cracknell [11–14], which are also described in Section 2 when compared with studies by Matsushima and co-researchers.

This chapter reviews former and state-of-the-art methods for estimating soil moisture by exploring the relationship between thermal inertia and soil moisture. Section 2 reviews past developments of methods for thermal inertia retrieval from land surface models. Section 3 describes how thermal inertia is experimentally observed, and how it is retrieved from land surface models in terms of the Xue and Cracknell-based models and the Matsushima models. Section 4 describes several semi-empirical parameterizations of thermal inertia in terms of soil moisture. Section 5 describes applications of thermal inertia for analyzing hydrometeorological phenomena around the Earth's surface and also discusses further exploration of thermal inertia itself and its applications. Section 6 presents conclusions.

2. Thermal inertia retrieval from energy balance models

Thermal inertia retrieval from an energy balance model of the Earth's surface began with a geological context in which different rocks or minerals respond differently to the incident solar radiation. Then, researchers' interests moved to the thermal inertia change according to soil moisture, which was coincident with the use of data obtained by sun-synchronous polar orbiting satellites that gave diurnal cycle of LSTs. Retrieval thermal inertia solely according to the soil moisture of the Earth's surface was developed during the last five decades. Most of the proposed methods employed the Fourier series of the LST diurnal variation, which was incorporated in a heat balance model of the Earth's surface.

A comprehensive model for retrieving thermal inertia using the energy balance model for the Earth's surface boundary conditions and the Fourier series for the diurnal change of the surface temperature was proposed by Price [3–5]. Price [6] made the terms of the turbulent heat flux (sensible and latent heat) simpler than previous studies to focus on retrieving thermal inertia. These studies used satellite LST measurements twice a day as the daily maximum and minimum LSTs, corresponding to daytime and nighttime, respectively, and substituted the LSTs into the first component (24-h period) of the Fourier series to calculate thermal inertia. Namely, they approximated the time-differential term of Eq. (7) as $\frac{\partial T(0,t)}{\partial t} \rightarrow \frac{\Delta T(0,t)}{\Delta t}$, where $\Delta T(0,t)$ is the difference between daily maximum and minimum LSTs, and Δt is the time difference of the two measurements.

Based on a series of studies performed by Price [3–6], Xue and Cracknell [11–14] proposed improved methods, which showed that data from satellites were good enough to accurately retrieve thermal inertia as well as using the time of the maximum LST. These models used the first- and second-order harmonics of the diurnal change (24- and 12-h periods) to fit the LST change considering the phase differences of both components to insolation. Thermal inertia was obtained from analytical but relatively complicated formulations. Based on the series of models proposed by Xue and Cracknell (hereinafter the XC model), several improved methods were proposed in terms of the timing of satellite measurements, actual timing of the diurnal maximum and minimum LSTs, and difference in LST change between daytime and nighttime. The details of the above schemes are described in Section 3.2.

Other than the above methods, Matsushima [15] applied the FRM to the surface heat balance model to retrieve thermal inertia. The FRM is also based on a sinusoidal boundary condition at the surface and the heat diffusion equation, which is essentially the same as the models based on the XC model. The Matsushima model [15] employed an FRM that was designed not only to mostly respond to the diurnal change but also to more rapid changes according to the temporal resolution of input the variables (insolation, air temperature, etc.). A change of the LST over a period of approximately a few hours was fairly reproduced by the FRM that had a characteristic period of 24 h, as illustrated in [16]. Similar results were found in other studies [2, 17], or higher-frequency nonsinusoidal forcing did not significantly affect the LST prediction [18]. This means that the FRM can reproduce temporal changes that have a wide range of LST frequencies via its relatively simple formulation. Using this method, the timing of satellite LST measurements was arbitrary in principle, irrespective of the daily maximum and minimum, but was more accurate for thermal inertia retrieval that the LSTs measured both in the daytime and in the nighttime, as shown in [19]. The accuracy of thermal inertia retrieval is improved if the coefficients of the atmospheric turbulent heat flux are set differently in the daytime and nighttime, as illustrated in [16]. The details are described in Section 3.2 when compared with the XC model.

3. Thermal inertia retrieval according to the spatial and temporal resolutions

3.1. A simple method using in-situ field measurements on a local scale

A simple method for estimating thermal inertia using simply measured surface radiative temperatures can be performed based on a finite difference form of Eq. (7), which is given as

$$\overline{G(0)} = \sqrt{\frac{P}{2\omega}}\left[\frac{\Delta T(0)}{\Delta t} + \omega\overline{T(0)}\right], \tag{10}$$

where $\Delta T(0)$ is a significant increase in LST during a relatively short-time span Δt (e.g., 30 min), $\overline{T(0)}$ is the temporal average of the LST difference from the soil temperature at infinite depths during the time span (practically, the daily average surface or air temperatures can be

used instead of the temperature at an infinite depth), and $\overline{G(0)}$ is soil heat flux at the surface averaged over the time span Δt. Matsushima et al. [20] estimated the thermal inertia of asphalt pavement based on Eq. (10) using data from $T(0)$ measured by a portable radiative thermometer approximately 1 m above the surface as well as a copper-constantan thermal couple on the surface and $\overline{G(0)}$ measured by a heat flux plate on the asphalt surface over 30 min under a summer daytime clear sky, assuming that the daily average thermocouple temperature was the temperature at an infinite depth. The results of the thermal inertia were 1140 J m^{-2} K^{-1} $s^{-1/2}$ and 1350 m^{-2} K^{-1} $s^{-1/2}$ using the LSTs measured by the portable radiative thermometer and the thermocouple, respectively. The values agree well with the standard value of 1220 m^{-2} K^{-1} $s^{-1/2}$ in the literature [21] (actually, this value is based on the volumetric heat capacity and thermal conductivity, calculated using the definition of thermal inertia Eq. (1)). The above result shows that thermal inertia can be estimated at a local scale using simple measurement equipment and also shows the feasibility of thermal inertia estimation using airborne and satellite thermal-infrared thermometry.

3.2. Model methods using multiple satellite data

Earth observing satellites are divided into polar-orbiting and geostationary. Both types have thermal-infrared bands to estimate LST. The temporal resolution of the geostationary satellites is superior to that of the polar-orbiting ones. By contrast, the spatial resolution and temperature accuracy of the geostationary satellites have been improving but are not yet superior to those of the polar-orbiting one [22, 23]. Therefore, in this section, models using polar-orbiting satellites are described and discussed.

Most of the models proposed so far for estimating thermal inertia were based on the model proposed by Xue and Cracknell [13] (XC model). This model is based on solving the thermal diffusion equation using the Fourier series expansion, which is described in Section 1. This model uses the first 24-h period and the second 12-h period Fourier harmonics of the sinusoidal components to reproduce the diurnal variation of LSTs. However, the two components were not always enough to reproduce an actual diurnal LST change. In these cases, the phase differences from the diurnal change of the insolation of respective components have to be adjusted. Measured values in thermal-infrared bands were used to calculate the LSTs. The LSTs are almost the daily maximum and minimum, which are suitable for accurately estimating thermal inertia. Various improvements were proposed based on the XC model. Among these improvements, a method using four satellite LSTs during a diurnal cycle irrespective of the daily maximum and minimum successfully retrieved thermal inertia [9]. Schemes for the phase and amplitude adjustments were also introduced. The phase adjustment was applied to the time-difference between the actual timing of the maximum and minimum LSTs and the overpass timings of the satellite measurements. This adjustment scheme was to have the satellite overpass timing approach the daily maximum or minimum LSTs using a cosine function for the phase difference when their estimated times were given [24]. On the other hand, an adjustment that decayed the LST amplitude after sunset was applied during nighttime due to the LST change being smaller than that in the daytime to avoid overestimating nighttime cooling [25]. These adjustments allowed arbitrary and many timings of the satellite

LSTs to be incorporated into the models for thermal inertia retrieval. The formulations for estimating thermal inertia were analytical but relatively complicated to describe and grasp. Moreover, various approximations were adopted to avoid the implicit formulations that required iterative calculations to retrieve thermal inertia. The input data required are according to individual models but are almost limited to the satellite LSTs, and some parameters with regard to the insolation are also required to specialize in retrieving thermal inertia from other parameters regarding the land surface processes. Models that simply address turbulent heat flux were proposed assuming that turbulent heat flux is proportional to the temperature difference between surface and atmosphere [26], or was ingeniously neglected [27]. Maltese et al. [10] proposed an XC-based model that only used the first Fourier component, which was enough to accurately retrieve thermal inertia using three LSTs during a diurnal cycle.

In contrast to the XC-based models, a series of models proposed by Matsushima and co-researchers (the most recent one is [16], hereafter referred to as M2018) was essentially based on the sinusoidal solution of the thermal diffusion equation. However, they adopted the FRM to avoid complicated analytical formulations for estimating thermal inertia while maintaining linearity. The FRM requires time integration to calculate the surface temperature as shown in Eq. (7). The characteristic frequency ω was set to the diurnal change (= $2\pi/86400(s^{-1})$) in M2018. Hence, the FRM appeared to be able to only reproduce the sinusoidal changes whose frequencies were near the characteristic frequency. However, shorter period changes were reproduced according to the input data changes shown in Figure 4 of M2018 because the force term (the time derivative term) was more temporally sensitive than the restore term (the product of the frequency and temperature difference from the daily average). The boundary conditions at the surface, the left side of Eq. (7), are also required. The boundary conditions are converted to the budget of net radiation, and sensible and latent heat at the surface using the heat balance equation. This requirement for the surface boundary conditions is as same as that of the XC-based models. M2018 was not specialized at retrieving thermal inertia, but other parameters with regard to the sensible and the latent heat flux, including the diurnal time series of insolation, air temperature, specific humidity, and wind speed, were required as input data. Also, the surface albedo and leaf area index were used as parameters, and the LSTs for the model optimization are described below. The above types of data were required, but all were readily available from satellite and meteorological data archives through the Internet, that is, a special observation was not needed. Instead of requiring many types of input data, the M2018 formulation was relatively simple and did not require phase and amplitude adjustments. The shift in values of the bulk transfer coefficients for the sensible and latent heat flux in the daytime and nighttime was required only to improve the accuracy of thermal inertia retrieval, which was approximately equivalent to the amplitude adjustment in the XC-based model by Schädlich et al. [25]. The time integration did not require an implicit scheme, but an optimization algorithm was required to retrieve thermal inertia and the other parameters at the same time. The optimization algorithm (the downhill simplex method that was employed in M2018) took time to retrieve parameters; hence, the M2018 had no advantage for the world-wide spatial scale and the temporal scale of several decades. In M2018, daily values of thermal inertia-derived soil moisture were estimated with a 3-km spatial resolution at $2^\circ \times 2^\circ$ in latitude and longitude using the 1-km spatial resolution of Moderate Resolution Imaging

Items	XC-based models	M2018 [16]
Basic equation	Differential equation of heat diffusion	
Boundary conditions	Sinusoidal function at the Earth's surface constant at infinite depth	
Model	Fourier series expansion	Two-source energy balance (TSEB) model based on force-restore model (FRM)
Solution	Fourier series components (first component only [10] or both first and second components [11–14] according to models)	Time integration of the respective surface temperatures of the two sources
Input data and parameters	LSTs parameters in terms of insolation parameters in terms of turbulent heat flux (according to the models)	LSTs insolation air temperature, specific humidity, wind speed albedo, and the leaf area index of the surface
Thermal inertia retrieval	Analytical solution	Model optimization (with other parameters regarding turbulent heat)
Number of diurnal LST measurements	Two (without timing adjustment for maximum and minimum [11–14]); two (with timing adjustment [24]); three or more [9, 10]	Arbitrarily determined (at least two—one in the daytime and the other in the nighttime—are suitable) [19]
Phase adjustment of LST	Needed in most models	Adjusted through time integration incorporating input time series

Table 1. Comparison of the differences between the XC-based models and M2018 model.

Spectroradiometer (MODIS) LST (MOD11_L2 and MYD11_L2). Thermal inertia retrieval at a 2-km resolution was, therefore, possible in principle [28].

Comparisons of the differences between the XC-based models and M2018 model are provided in **Table 1**.

4. How soil moisture is derived from thermal inertia

4.1. Combination of $C-\theta$ and $\lambda-\theta$ relations

One of the principal methods for deriving the relationship between thermal inertia P and soil moisture (volumetric water content in most cases) θ uses the definition of thermal inertia $P=\sqrt{c\rho\lambda}=\sqrt{C\lambda}$. Specifically, the effective models for using soil moisture to determine the volumetric heat capacity and thermal conductivity, respectively, proposed by de Vries [29] were used in several thermal inertia models [7, 8]. The volumetric heat capacity is formulated as

$$C=C_w\theta+C_m(1-\theta_*), \tag{11}$$

where C_w and C_m are the volumetric heat capacities of water and minerals, respectively, and θ_* is the soil moisture at saturation, in other words, the porosity of the soil, and the thermal conductivity λ is formulated as

$$\lambda = \sum_{i=0}^{N} K_i X_i \lambda_i / \sum_{i=0}^{N} K_i X_i, \tag{12}$$

where N is the number of types of granules and particles that make up the soil, including the minerals, organic matter, water, and air inside the soil. Each component has a thermal conductivity λ_i and a volume fraction X_i, and K_i is a weighting factor that is the ratio of the average temperature gradient in the granules of the i-th component to the average temperature gradient in the medium. See Appendix for details on the formulation of K_i. Minacapilli et al. [30] combined the linear relation of the volumetric heat capacity proposed by de Vries [29] and an empirical parameterization for thermal conductivity proposed by Lu et al. [31] to derive thermal inertia. The proposed models for the thermal conductivity of unsaturated soil have been expanded, and the details are provided in a review by Dong et al. [32].

Ma and Xue [33] proposed an empirical parameterization that often appears in the literature. This parameterization calculates thermal inertia for a given soil moisture (gravimetric soil water content) when the soil (mineral) density and water density are known.

Noilhan and Planton [34] derived the relationship between thermal inertia and soil moisture in another way. This method was basically a combination of thermal inertia, the relationship between soil moisture and matric potential of soil, and a parameterization of the thermal conductivity as a function of the matric potential proposed by McCumber and Pielke [35]. In their paper, they showed the relationship between soil moisture and soil thermal coefficient C_s, which was defined in their paper, but was able to be rearranged to according to the relationship between M2018 thermal inertia and soil moisture, which is formulated as

$$C_s = \frac{2}{P\sqrt{\tau/\pi}}, \tag{13}$$

and

$$C_s = C_{s,*}\left[\frac{\theta_*}{\max(\theta, \theta_w)}\right]^{(2\ln 10/b)}, \tag{14}$$

where $\tau = 2\pi/\omega$, and subscripts * and w denote the saturation and wilting points, respectively. Substituting Eq. (13) into Eq. (14), after several calculations, yields

$$\theta = sP^{(2\ln 10/b)} \tag{15}$$

where

$$s = \theta_*\left(\frac{C_{s,*}}{2}\sqrt{\frac{\tau}{\pi}}\right)^{(2\ln 10/b)} \tag{16}$$

The constant s depends on the parameters b, θ_*, and $C_{s,*}$, of the Clapp and Hornberger parameterization [36]. In particular, parameter b is related to 11 categories of soil types

determined by the United States Department of Agriculture (USDA), and parameter b is a predictive parameter of the clay ratio in soil [37].

4.2. Analogous to Johansen's thermal conductivity model

Johansen [38] proposed a model for determining thermal conductivity as a function of soil moisture. The concept of the model is that thermal conductivity is formulated as a universal function of soil moisture and that the function shape is determined by parameters of the formulation. The parameters are determined according to the soil type, such as sand, loam, silt, and clay. The generalized form of the parameterization is given as

$$\lambda = \lambda_{dry} + \left(\lambda_* - \lambda_{dry}\right)K_p \tag{17}$$

where the subscript *dry* denotes zero soil moisture, and K_p is the universal Kersten function. The formulation is defined as a function of soil moisture from zero to the saturation point (porosity). Then, the problem is reduced to determine the specific formulation and its parameter values. The specific form of the Kersten function is a power function, and the curve shape depends on the power according to the soil type, which has strong nonlinearity in most cases.

Murray and Verhoef [39] applied the above Johansen type model to thermal inertia parameterization as follows:

$$P = P_{dry} + \left(P_* - P_{dry}\right)K_p \tag{18}$$

To calculate the thermal inertia value, parameters P_{dry} and P_* have to be determined, and the formulation of K_p is given as the parameterization proposed by Lu et al. [31] in [39], as

$$K_p = \exp\left[\gamma\left(1 - S_r^{\gamma-\delta}\right)\right], \tag{19}$$

where γ and δ are the coefficients for optimization according to the soil type, and S_r is the soil moisture normalized by saturation. Lu et al. [40] proposed a similar parameterization as that in [39]. Minacapilli et al. [41] tested the performance of the Murray and Verhoef model [39] and extended the Johansen model concept to the apparent thermal inertia. Recently, Lu et al. [42] showed that P_{dry} was parameterized as a function of porosity, in other words, the soil clay ratio, improving the accuracy of thermal inertia retrieval.

Again, thermal inertia is the square root of the product of volumetric heat capacity and thermal conductivity, and volumetric heat capacity increases modestly according to soil moisture. By contrast, thermal conductivity has strong nonlinearity compared to soil moisture. Therefore, thermal inertia can be formulated as a nonlinear function, and even, the square root operates the product $C\lambda$. Lu et al. [40] applied the formulation to thermal inertia and determined the parameter values according to three soil types. The minimum and maximum thermal inertia values range over soil moisture from zero to saturation. If some amount of error is added to the retrieved value of thermal inertia from a model calculation or laboratory experiment, the value may be less than the minimum, and hence, soil moisture cannot be calculated due to K_p being negative.

5. Applications and discussion for future exploration

5.1. Advantages and disadvantages compared to microwave-based methods

Thermal inertia-derived soil moisture can be estimated by combining methods as described in Sections 3 and 4. An advantage of the thermal inertia method that uses satellite data is that the spatial resolution is a couple of kilometers, which is much more precise than that of the microwave-based method, which has the spatial resolution of several tens of kilometers. However, there are also disadvantages, such as the precision and accuracy of thermal inertia retrieval being affected by the sky conditions, especially clouds, which are the weakest point in using the thermal-infrared bands. A recent study showed that the microwave brightness temperatures complemented the thermal-infrared derived LST, but instead of this, the spatial resolution of the thermal-infrared LST had to be sacrificed [43]. Another disadvantage is that the thermal inertia of a surface covered with dense vegetation is difficult to retrieve. Soil moisture retrieval using the microwave bands also has the same problem. Thermal inertia retrieval over a surface covered with sparse vegetation has been achieved in many studies in which M2018 is categorized in the two-source energy balance (TSEB) concept [44, 45]. In M2018, the vegetation canopy is modeled according to its surface temperature, the three parameters that should be optimized, and the leaf area index, which is given as satellite data. The effectiveness of the TSEB model is not only to retrieve thermal inertia but also possibly to accurately calculate heat flux with regard to the surface heat balance. The denser the vegetation, the less accurate the thermal inertia retrieval. It should be noted that the thermal inertia-derived soil moisture is calculated through a simple TSEB model as well as the surface heat flux, including evapotranspiration.

According to the above advantages and disadvantages, soil moisture derivation for a surface is more effective in arid and semi-arid regions where clear sky conditions overwhelm other conditions and where there are spatial soil moisture contrasts, for example, between an oasis and other land cover, as well as significant temporal changes, for example, from just after to approximately 1 week after a rainfall.

The optimization scheme for the thermal inertia retrieval is crucial to save calculation time. M2018 uses the downhill simplex method [46], which is generally suitable for optimizing less than approximately five parameters. It takes approximately 20–40 s to retrieve seven parameters including the thermal inertia of one grid in M2018 using a workstation. The downhill simplex method has the advantage of not diverging in the optimizing process, but the algorithm is not simple and requires a long time to complete. A more efficient optimization scheme needs to be explored.

5.2. Assimilation with microwave-based data

Data assimilation procedures are downscaled schemes of microwave-based soil moisture, which has a scale of several tens of kilometers, to one to a couple of kilometers. These schemes have recently been improved [47–50] using visible, near-infrared, and thermal-infrared satellite data, which have more precise spatial resolution than microwaves. These procedures can be

competitive with thermal inertia procedures to derive surface soil moisture. However, one weak point with regard to microwave-based soil moisture (soil moisture active passive: SMAP) was noted, and it was a dry down process occurred after an antecedent rainfall that was too rapid for in-situ soil moisture measurement [50]. By contrast, the thermal inertia-derived soil moisture agreed fairly well with the in-situ soil moisture found in several dry down processes (M2018). This agreement may be because the sensing depth of the surface microwave-based soil moisture was shallower than the in-situ measurement and sensitive to the soil moisture itself [51], whereas the representative depth scale of the FRM is not as sensitive to soil moisture and almost agrees with the in-situ measuring depth (M2018). Regarding the spatial resolution of the satellite sensors, an Earth observing satellite with a more precise spatial resolution in the visible, near-infrared, and thermal-infrared bands, the Global Change Observation Mission-Climate (GCOM-C), was recently launched in 2017 by the Japan Aerospace Exploration Agency (JAXA), and the data will be available for general use within 1 year. Its LST spatial resolution is 500 m, twice than that of the MODIS resolution, which will benefit both data assimilation and thermal inertia procedures. Another GCOM-C type satellite will hopefully be able to be operated like MODIS. On the other hand, microwave-based soil moisture can be obtained almost every day regardless of the sky conditions (leading to partial lack of data in some regions due to the satellite orbit). There are trade-offs that have between the above described advantages and disadvantages of the respective procedures.

The Global Satellite Mapping of Precipitation (GSMaP) [52] operated by JAXA is a system that measures the spatio-temporal distribution of precipitation at the Earth's surface on a 0.1°-spatial scale and a 1-hour temporal scale, and the latest data are added every hour. In arid and semi-arid regions far from rivers, short-term discharge and infiltration should be negligible, accordingly the water budget is calculated using the thermal inertia-derived soil moisture and GSMaP precipitation. Currently, there is not adequate accuracy for both variables to calculate a water budget, but it is worth tackling this issue to estimate regional water cycles and resources.

5.3. Dust emission

Dust emissions in arid and semi-arid regions have posed serious problems such as soil nutrition loss, crop and vegetation damage, and air quality deterioration. Dust emissions, for example, from Northeast Asia, influence not only individual arid or semi-arid regions but also regions across national boundaries and seas because some dust is raised by strong atmospheric convection and carried by strong westerly winds [53]. Dust emission from the Saharan Desert often harms the surrounding regions including regions far from Africa [53]. Wind erosion from agricultural land often causes local and regional problems according to tillage practices [54]. To predict these dust emissions in advance, monitoring and prediction of the surface soil moisture distribution over an area where dust emission occurrences are concentrated are important. Scheidt et al. [24] examined the spatial distribution of thermal inertia for five soil types in a desert of approximately 20 km using eight couples of the daytime and nighttime thermal-infrared surface temperatures observed by the Advanced Spaceborne Thermal Emission and Reflection (ASTER) and MODIS and then estimated the threshold wind speed based

on the estimated thermal inertia values after Fécan [55]. The threshold wind speed or friction velocity for dust emissions according to surface soil moisture was examined using carefully designed wind tunnel experiments with multiple soil types, and the threshold friction velocity was found to be related to the soil matric potential and not aligned with the gravimetric soil moisture for the examined soil types [55–58]. The matric potential is not as readily available as the soil moisture, otherwise the function connecting the two variables is known in advance. Considering that it should be difficult to obtain the relationship between thermal inertia and matric potential, and practical relationships between thermal inertia-derived soil moisture and threshold wind speed with regard to individual soil types are required.

In the region where the Earth's surface and subsurface are seasonally frozen, dust emissions begin to occur (early spring) when only the surface is melted and dry but not the subsurface just beneath a thin surface layer. The thermal inertia at the representative depth is still affected by the frozen soil, but the surface radiative temperature is highly positive in degrees Celsius due to the dried surface, which is suitable for dust emission (in other words, high erodibility) if the wind is necessarily strong. The temperature difference was up to at most 20°C (unpublished result). Dust emission is likely to occur in early spring when the meteorological conditions are likely to be windy; however, an empirical relationship between thermal inertia-derived soil moisture and threshold wind speed using observations during spring to early autumn [28] is difficult to apply because thermal inertia is likely to be underestimated in early spring possibly due to the large difference between the surface and the subsurface temperatures. There is no common formulation for thermal inertia-derived soil moisture with regard to the threshold wind speed in early spring or other seasons.

5.4. Water budget and management

Monitoring the spatial distribution of surface soil moisture over a wide agricultural area is required for optimal water management. An example presented by Minecapllia et al. [30] showed the spatial distribution of thermal inertia over a small-scale cultivated field using airborne thermal images taken in the daytime and nighttime.

Root zone soil moisture has been examined in several studies [50, 59], using a thermal inertia procedure with the FRM applied to the soil water transport and data assimilation procedures, respectively. All of the studies noted that the initial values of the root zone soil moisture were significant for reducing the simulation error. It was noted that the FRM applied to soil moisture was not straight-forward like the soil temperature because of the nonlinearity in soil water transport that representatively appeared in the Richards equation [34, 59]. Various processes of water transport in soil such as infiltration, redistribution, and vapor transport should be improved [60].

The precise spatial resolution of satellite LST is better used for coinciding topography or land use on approximately a 1-km scale. Overlaying or assimilating thermal inertia-derived soil moisture over a common scale of topography or land use in the range of a watershed should contribute to the water budget estimation (discharge, infiltration, and evapotranspiration) when precipitation is known. If agricultural land use is resolved at a 1-km resolution, it is

practically suitable for estimating thermal inertia and its applications using M2018 with GCOM-C LST.

6. Conclusions

A vast number of studies have been proposed for estimating soil moisture, and thermal inertia-based methods have been improving for the last five decades. These methods are based on the thermal diffusion equation combined with sinusoidal function boundary conditions at the Earth's surface and are constant at an infinite depth. There are two solutions for retrieving thermal inertia of which both use satellite thermal-infrared-based LST. One uses the Fourier series expansion, and the other employs the force-restore method. There are advantages and disadvantages in their formulation, calculation procedures, time, and adjustment schemes; however, both solutions are essentially the same in principle. The parameterization for converting thermal inertia to soil moisture is also important. Two ways to perform this parameterization have been proposed. One uses the relationships of soil moisture to the volumetric heat capacity and thermal conductivity, and the other is analogous to the Johansen type thermal conductivity model. The individual studies proposed so far combined a method for retrieving thermal inertia and parameterization for converting it to soil moisture. The accuracy of estimating surface soil moisture for individual studies was not significantly different. The current and future applications of thermal inertia-derived soil moisture are discussed. The thermal inertia approach will be competitive with the assimilation method combining microwave-based soil moisture and satellite data from the other wavelength bands (visible, near-infrared, and thermal-infrared). There are advantages and disadvantages to both approaches in regard to spatial resolution, sky conditions, and the dry down process. Issues to be tackled remain for dust emission processes, especially in relation to soil moisture. Regional water budgeting and management can be applied to arid land water resource and agricultural practice considering the fusion of other satellite data such as GSMaP precipitation.

Acknowledgements

This chapter is based on an aggregation of contributions from personal collaborations and research groups. This chapter is also partly supported by JSPS KAKENHI Grant Number JP 26289159.

Appendix

Details of the weighting factor K_i formulation in Section 3.

Details of the formulation of K_i are given as

$$K_i = \frac{1}{3}\sum_{j=1}^{3}\left[1+\left(\frac{\lambda_i}{\lambda_0}-1\right)g_{ij}\right]^{-1}, \tag{20}$$

where λ_0 is the conductivity of the medium and g_{ij} is a shape factor that takes into account the shape and orientation of the granules. Since $\sum_{j=1}^{3} g_{ij} = 1$ and a spheroidal shape is assumed $(g_{i1} = g_{i2})$, the above equation reduces to:

$$K_i = \frac{2}{3\left[1+\left(\frac{\lambda_i}{\lambda_0}-1\right)g_i\right]} + \frac{1}{3\left[1+\left(\frac{\lambda_i}{\lambda_0}-1\right)(1-2g_i)\right]}. \tag{21}$$

Author details

Dai Matsushima

Address all correspondence to: matsushima.dai@it-chiba.ac.jp

Chiba Institute of Technology, Narashino, Chiba, Japan

References

[1] van Wijik WR, de Vries DA. Periodic temperature variations in a homogeneous soil. In: van Wijik WR, editor. Physics of Plant Environment. Amsterdam: North-Holland Publ. Co.; 1963. pp. 103-143

[2] Deardorff JW. Efficient prediction of ground surface temperature and moisture, with inclusion of a layer of vegetation. Journal of Geophysical Research. 1978;**83**:1889-1903. DOI: 10.1029/JC083iC04p01889

[3] Price JC. Thermal inertia mapping: A new view of the earth. Journal of Geophysical Research. 1977;**82**:2582-2590. DOI: 10.1029/JC082i018p02582

[4] Price JC. The potential of remotely sensed thermal infrared data to infer surface soil moisture and evaporation. Water Resources Research. 1980;**16**:787-795. DOI: 10.1029/WR016i004p00787

[5] Price JC. Estimating surface temperatures from satellite thermal infrared data—A simple formulation for the atmospheric effect. Remote Sensing of Environment. 1983;**13**:353-361. DOI: 10.1016/0034-4257(83)90036-6

[6] Price JC. On the analysis of thermal infrared imagery: The limited utility of apparent thermal inertia. Remote Sensing of Environment. 1985;**18**:59-73. DOI: 10.1016/0034-4257(85)90038-0

[7] Pratt DA, Ellyett CD. The thermal inertia approach to mapping of soil moisture and geology. Remote Sensing of Environment. 1979;**8**:151-168. DOI: 10.1016/0034-4257(79)90014-2

[8] van de Griend AA, Camillo PJ, Gurney RJ. Discrimination of soil physical parameters, thermal inertia, and soil moisture from diurnal surface temperature fluctuations. Water Resources Research. 1985;**21**:997-1009. DOI: 10.1029/WR021i007p00997

[9] Sobrino JA, El Kharraz MH. Combining afternoon and morning NOAA satellites for thermal inertia estimation: 1. Algorithm and its testing with hydrologic atmospheric pilot experiment-Sahel data. Journal of Geophysical Research. 1999;**104**:9445-9453. DOI: 10.1029/1998JD200109

[10] Maltese A, Bates PD, Capodici F, Cannarozzo M, Ciraolo G, La Loggia G. Critical analysis of thermal inertia approaches for surface soil water content retrieval. Hydrological Sciences Journal. 2013;**58**:1144-1161. DOI: 10.1080/02626667.2013.802322

[11] Xue Y, Cracknell AP. Thermal inertia mapping: From research to operation. In: Cracknelll AP, Vaughan RA, editors. Proceedings of the 18th Annual Conference of the Remote Sensing Society; 15–17 September 1992; University of Dundee. Nottingham, UK: Remote Sensing Society; 1992. pp. 471-480

[12] Xue Y, Cracknell AP. Advanced thermal inertia modelling and its application: Modelling emissivity of the ground. In: Proceedings of the 25th International Symposium on Remote Sensing and Global Environmental Change; 4–8 April 1993; Graz, Austria. Ann Arbor: ERIM; 1993. pp. II-121-II-122

[13] Xue Y, Cracknell AP. Advanced thermal inertia modelling. International Journal of Remote Sensing. 1995;**16**:431-446. DOI: 10.1080/01431169508954411

[14] Cracknell AP, Xue Y. Dynamic aspects of surface temperature from remotely-sensed data using advance thermal inertia model. International Journal of Remote Sensing. 1996;**17**: 2517-2532. DOI: 10.1080/01431169608949090

[15] Matsushima D. Estimating regional distribution of surface heat fluxes by combining satellite data and a heat budget model over the Kherlen River Basin, Mongolia. Journal of Hydrology. 2007;**333**:86-99. DOI: 10.1016/j.jhydrol.2006.07.028

[16] Matsushima D, Asanuma J, Kaihotsu I. Thermal inertia approach using a heat budget model to estimate the spatial distribution of surface soil moisture over a semi-arid grassland in Central Mongolia. Journal of Hydrometeorology. 2018;**19**:245-265. DOI: 10.1175/JHM-D-17-0040.1

[17] Dickinson RE. The force-restore model for surface temperatures and its generalizations. Journal of Climate. 1988;**1**:1086-1097. DOI: 10.1175/1520-0442(1988)001<1086:TFMFST>2.0.CO;2

[18] Hirota T, Pomeroy JW, Granger RJ, Maule CP. An extension of the force-restore method to estimating soil temperature at depth and evaluation for frozen soils under snow. Journal of Geophysical Research. 2002;**107**:ACL 11-1-ACL 11-10. DOI: 10.1029/2001JD001280

[19] Matsushima D, Kimura R, Shinoda M. Soil moisture estimation using thermal inertia: Potential and sensitivity to data conditions. Journal of Hydrometeorology. 2012;**13**:638-648. DOI: 10.1175/JHM-D-10-05024.1

[20] Matsushima D, Sensui Y, Ryuzaki T, Misaka I, Ando K, Yokoyama H, Narita K. A study on thermal environmental assessment in a street space: 1. Estimating heat storage in the subsurface and buildings using data from surface temperature measurements. In: Proceedings of the Annual Meeting of Architectural Institute of Japan; 26–29 August 2009; Sendai. Tokyo: Architectural Institute of Japan; 2009. pp. 729-730

[21] Tanaka S, Takeda H, Tsuchiya T, Iwata T, Terao M. Architectural Environmental Engineering. 3rd ed. Tokyo: Inoue Shoin; 2006. p. 324

[22] Anderson MC, Kustas WP, Norman JM, Hain CR, Mecikalski JR, Schultz L, et al. Mapping daily evapotranspiration at field to continental scales using geostationary and polar orbiting satellite imagery. Hydrology and Earth System Sciences. 2011;**15**:223-239. DOI: 10.5194/hess-15-223-2011

[23] Wu P, Shen H, Zhang L, Göttsche FM. Integrated fusion of multi-scale polar-orbiting and geostationary satellite observations for the mapping of high spatial and temporal resolution land surface temperature. Remote Sensing of Environment. 2015;**156**:169-181. DOI: 10.1016/j.rse.2014.09.013

[24] Scheidt S, Ramsey M, Lancaster N. Determining soil moisture and sediment availability at White Sands Dune Field, New Mexico, from apparent thermal inertia data. Journal of Geophysical Research. 2010;**115**:F02019. DOI: 10.1029/2009JF001378

[25] Schädlich S, Göttsche FM, Olesen FS. Influence of land surface parameters and atmosphere on METEOSAT brightness temperatures and generation of land surface temperature maps by temporally and spatially interpolating atmospheric correction. Remote Sensing of Environment. 2001;**75**:39-46. DOI: 10.1016/S0034-4257(00)00154-1

[26] Cai G, Xue Y, Hu Y, Wang Y, Guo J, Luo Y, Wu C, Zhong S, Qi S. Soil moisture retrieval from MODIS data in Northern China Plain using thermal inertia model. International Journal of Remote Sensing. 2007;**28**:3567-3581. DOI: 10.1080/01431160601034886

[27] Verhoef A. Remote estimation of thermal inertia and soil heat flux for bare soil. Agricultural and Forest Meteorology. 2004;**123**:221-236. DOI: 10.1016/j.agrformet.2003.11.005

[28] Matsushima D, Kimura R, Kurosaki Y, Shinoda M. A method for estimating the threshold wind speed as a function of soil moisture in a local scale using multiple models and data archives. (in Preparation)

[29] de Vries DA. Thermal properties of soils. In: Van Wijik WR, editor. Physics of Plant Environment. New York: Wiley; 1963. pp. 210-235

[30] Minacapilli M, Iovino M, Blanda F. High resolution remote estimation of soil surface water content by a thermal inertia approach. Journal of Hydrology. 2009;**379**:229-238. DOI: 10.1016/j.jhydrol.2009.09.055

[31] Lu S, Ren T, Gong Y, Horton R. An improved model for predicting soil thermal conductivity from water content at room temperature. Soil Science Society of America Journal. 2007;**71**:8-14. DOI: 10.2136/sssaj2006.0041

[32] Dong Y, McCartney JS, Lu N. Critical review of thermal conductivity models for unsaturated soils. Geotechnical and Geological Engineering. 2015;**33**:207-221. DOI: 10.1007/s10706-015-9843-2

[33] Ma AN, Xue Y. A study of remote sensing information model of soil moisture. In: Proceedings of the 11th Asian Conference on Remote Sensing, I. 15–21 November 1990; Beijing; 1990. pp. P-11-1-P-11-5

[34] Noilhan J, Planton S. A simple parameterization of land surface processes for meteorological models. Monthly Weather Review. 1989;**117**:536-549. DOI: 10.1175/1520-0493(1989)117<0536:ASPOLS>2.0.CO;2

[35] McCumber MC, Pielke RA. Simulation of the effects of surface fluxes of heat and moisture in a mesosclae numerical model: 1. Soil layer. Journal of Geophysical Research. 1981;**86**:9929-9938. DOI: 10.1029/JC086iC10p09929

[36] Clapp RB, Hornberger GM. Empirical equations for some soil hydraulic properties. Water Resources Research. 1978;**14**:601-604. DOI: 10.1029/WR014i004p00601

[37] Cosby BJ, Hornberger GM, Clapp RB, Ginn TR. A statistical exploration of the relationships of soil moisture characteristics to the physical properties of soils. Water Resources Research. 1984;**20**:682-690. DOI: 10.1029/WR020i006p00682

[38] Johansen O. Thermal conductivity of soils [PhD thesis]. University of Trondheim; 1975

[39] Murray T, Verhoef A. Moving tiwards a more mechanistic approach in the determination of soil heat flux from remote measurements: I. A universal approach to calculate thermal inertia. Agricultural and Forest Meteorology. 2007;**147**:80-87. DOI: 10.1016/j.agrformet.2007.07.004

[40] Lu S, Ju Z, Ren T, Horton R. A general approach to estimate soil water content from thermal inertia. Agricultural and Forest Meteorology. 2009;**149**:1693-1698. DOI: 10.1016/j.agrformet.2009.05.011

[41] Minacapilli M, Cammalleri C, Ciraolo G, D'Asaro F, Iovino M, Maltese A. Thermal inertia modelling for soil surface water content estimation: A laboratory experiment. Soil Science Society of America Journal. 2012;**76**:92-100. DOI: 10.2136/sssaj2011.0122

[42] Lu Y, Horton R, Zhang X, Ren T. Accounting for soil porosity improves a thermal inertia mode for estimating surface soil water content. Remote Sensing of Environment. 2018;**212**:79-89. DOI: 10.1016/j.rse.2018.04.045

[43] Holmes TRH, Hain CR, Anderson MC, Crow WT. Cloud tolerance of remote-sensing technologies to measure land surface temperature. Hydrology and Earth System Sciences. 2016;**20**:3263-3275. DOI: 10.5194/hess-20-3263-2016

[44] Kondo J, Watanabe T. Studies on the bulk transfer coefficients over a vegetated surface with a multilayer energy budget model. Journal of the Atmospheric Sciences. 1992;**49**: 2183-2199. DOI: 10.1175/1520-0469(1992)049<2183:SOTBTC>2.0.CO;2

[45] Norman JM, Kustas WP, Humes KS. A two-source approach for estimating soil and vegetation energy fluxes in observations of directional radiometric surface temperature. Agricultural and Forest Meteorology. 1995;**77**:263-293. DOI: 10.1016/0168-1923(95)02265-Y

[46] Nelder JA, Mead R. A simplex method for function minimization. Computer Journal. 1965;**7**:308-313. DOI: 10.1093/comjnl/7.4.308

[47] Sawada Y, Koike T, Walker JP. A land data assimilation system for simultaneous simulation of soil moisture and vegetation dynamics. Journal of Geophysical Research – Atmospheres. 2015;**120**:5910-5930. DOI: 10.1002/2014JD022895

[48] Sawada Y, Koike T. Towards ecohydrological drought monitoring and prediction using a land data assimilation system: A case study on the horn of Africa drought (2010–2011). Journal of Geophysical Research – Atmospheres. 2016;**121**:8229-8242. DOI: 10.1002/2015JD024705

[49] Sawada Y, Koike T, Aida K, Toride K, Walker JP. Fusing microwave and optical satellite observations to simultaneously retrieve surface soil moisture, vegetation water content, and surface soil roughness. IEEE Geoscience and Remote Sensing. 2017;**55**:6195-6206. DOI: 10.1109/TGRS.2017.2722468

[50] Bandara R, Walker JP, Rüdiger C, Merlin O. Towards soil property retrieval from space: An application with disaggregated satellite observations. Journal of Hydrology. 2015;**522**: 582-593. DOI: 10.1016/j.jhydrol.2015.01.018

[51] Shellito PJ, Small EE, Colliander A, Bindlish R, Cosh MH, Berg AA, Bosch DD, Caldwell TG, Goodrich DC, McNairn H, Prueger JH, Starks PJ, van der Velde R, Walker JP. SMAP soil moisture drying more rapid than observed in situ following rainfall events. Geophysical Research Letters. 2016;**43**:8068-8075. DOI: 10.1002/2016GL069946

[52] Kubota T, Shige S, Hashizume H, Aonashi K, Takahashi N, Seto S, Hirose M, Takayabu YN, Ushio T, Nakagawa K, Iwanami K, Kachi M, Okamoto K. Global precipitation map using satellite-borne microwave radiometers by the GSMaP project: Production and validation. IEEE Geoscience and Remote Sensing. 2007;**45**:2259-2275. DOI: 10.1109/TGRS.2007.895337

[53] Shao Y. Physics and Modelling of Wind Erosion. 2nd Revised and Expanded ed. Berlin: Springer; 2008. 452p

[54] Sharratt BS, Collins HP. Wind Erosion potential influenced by tillage in an irrigated potato–sweet corn rotation in the Columbia Basin. Agronomy Journal. 2018;**110**:842-849. DOI: 10.2134/agronj2017.12.0681

[55] Fécan F, Marticorena B, Bergametti G. Parametrization of the increase of the aeolian erosion threshold wind friction velocity due to soil moisture for arid and semi-arid areas. Annales Geophysicae. 1999;**17**:149-157. DOI: 10.1007/s00585-999-0149-7

[56] McKenna-Neuman C, Nickling WG. A theoretical and wind tunnel investigation of the effect of capillary water on the entrainment of sediment by wind. Canadian Journal of Soil Science. 1989;**69**:79-96. DOI: 10.4141/cjss89-008

[57] Sharratt BS, Vaddella VK, Feng G. Threshold friction velocity influenced by wetness of soils within the Columbia Plateau. Aeolian Research. 2013;**9**:175-182. DOI: 10.1016/j.aeolia.2013.01.002

[58] Sharratt BS, Vaddella V. Threshold friction velocity of crusted windblown soils in the Columbia Plateau. Aeolian Research. 2014;**15**:227-234. DOI: 10.1016/j.aeolia.2014.08.002

[59] Verstraeten WW, Veroustraete F, van der Sande CJ, Grootaers I, Feyen J. Soil moisture retrieval using thermal inertia, determined with visible and thermal spaceborne data, validated for European forests. Remote Sensing of Environment. 2006;**101**:299-314. DOI: 10.1016/j.rse.2005.12.016

[60] Or D, Lehmann P, Shahraeeni E, Shokri N. Advances in soil evaporation physics—A review. Vadose Zone Journal. 2013;**12**. DOI: 10.2136/vzj2012.0163